IOP Publishing New J. Phys. 24 (2022) 123013 https://doi.org/10.1088/1367-2630/aca8c7

New Journal of Physics
The open access journal at the forefront of physics

Deutsche Physikalische Gesellschaft DPG
IOP Institute of Physics

Published in partnership with: Deutsche Physikalische Gesellschaft and the Institute of Physics

OPEN ACCESS

RECEIVED
22 September 2022

REVISED
18 November 2022

ACCEPTED FOR PUBLICATION
5 December 2022

PUBLISHED
15 December 2022

PAPER

Recoil experiments determine the eigenmodes of viscoelastic fluids

Félix Ginot[1], Juliana Caspers[2], Luis Frieder Reinalter[1], Karthika Krishna Kumar[1], Matthias Krüger[2] and Clemens Bechinger[1,*]

[1] Fachbereich Physik, Universität Konstanz, 78457 Konstanz, Germany
[2] Institute for Theoretical Physics, Georg-August Universität Göttingen, 37073 Göttingen, Germany
[*] Author to whom any correspondence should be addressed.

E-mail: clemens.bechinger(at)uni-konstanz.de

Keywords: viscoelasticity, transient microrheology, non-Markovian, optical tweezers, colloids

Supplementary material for this article is available online

Abstract

We experimentally investigate the transient recoil dynamics of a colloidal probe particle in a viscoelastic fluid after the driving force acting on the probe is suddenly removed. The corresponding recoil displays two distinct timescales which are in excellent agreement with a microscopic model which considers the probe particle to be coupled to two bath particles via harmonic springs. Notably, this model exhibits two sets of eigenmodes which correspond to reciprocal and non-reciprocal force conditions and which can be experimentally confirmed in our experiments. We expect our findings to be relevant under conditions where particles are exposed to non-steady shear forces as this is encountered e.g. in microfluidic sorting devices or the intermittent motion of motile bacteria within their natural viscoelastic surrounding.

1. Introduction

The mechanical response of small objects which are driven with external forces or self-propel through viscoelastic fluids, e.g. micelles, networks of (bio)polymers or colloidal suspensions is of central importance for many natural phenomena and applications. Since typical relaxation times of the microstructure of viscoelastic materials can be on the order of several seconds, this leads to non-trivial behaviors for microscopic probes when sheared through such systems. Typically, probe particles are driven either by constant or oscillating external forces which then allows to obtain insights into the non-linear mechanical response of such systems [1–6]. However, so far hardly any theoretical description exists for driving conditions which may be relevant in non-steady flows within microfluidic devices or the intermittent motion of living organisms. Several experimental and theoretical studies reported a rich transient recoil dynamics when the driving force of colloidal particles sheared through different types of complex fluids is suddenly removed [7–11]. Because similar recoil behaviors have been found in wormlike micelles, polymer solutions, and entangled λ-phage DNA, this suggests a general, material-independent description which, however, is currently not available.

In this work we experimentally investigate the relaxation (recoil) of a colloidal bead after driving it through a wormlike micellar solution with an optical tweezers and then suddenly turning it off (particle release). Independent of the shearing protocol, we observe that the recoil always proceeds via a double-exponential relaxation process. Notably, the timescales during relaxation are not identical compared to those characteristic under shearing conditions which are also accessible in our experiments. Our results are in quantitative agreement with a generic microscopic model where the response of the fluid is described with two *bath* particles connected by linear springs to the probe. The characteristic timescales on which micro particles respond to viscoelastic fluids strongly depend on the specific choice of the shearing protocol, partial loading or relaxation of the system will strongly suppress the long and short timescale respectively.

Lastly, this model naturally has two sets of eigenmodes, corresponding to reciprocal (trap off) and nonreciprocal forces (trap on) and which are both confirmed in our experiments.

2. Experimental setup

In our experiments we used a viscoelastic solution of 5 mM equimolar cetylpyridinium chloride monohydrate (CPyCl) and sodium salicylate (NaSal) to which we added a small amount of silica probe particles with diameter $2r = 2.73\,\mu$m. The solution was contained in a sealed sample cell with 100 μm height being kept at a temperature of 25 °C. Under such conditions, the fluid forms an entangled network of giant worm-like micelles with pronounced viscoelastic properties [12]. In this semi-dilute regime (the critical micellar concentration is ∼4 mM), they act as 'equilibrium polymers' and are known to be well described by a Maxwell model being characterized by a single relaxation time [13, 14]. We note, however, that the relaxation process can be more complex at higher concentrations [15, 16] and in other systems [17–20]. The colloidal probe was optically trapped in the focus of a Gaussian laser beam $\lambda = 1064$ nm using a high magnification microscope objective (100× oil immersion, NA = 1.45). This yielded a rather stiff trap with trapping strength $\kappa_{\mathrm{OT}} = 32 \pm 1\,\mu\mathrm{N\,m^{-1}}$. To avoid possible interactions with the sample walls, the trap was located at least 30 μm away from any surface. Motion of the probe relative to the fluid has been achieved by translating the sample cell with constant velocity using a computer controlled piezo-driven stage. This motion has been synchronized with the laser intensity to realize different shearing protocols as described in detail below. Pictures of the probe particles have been recorded by video microscopy with a frame rate of 100 Hz. Using a custom Matlab [21] algorithm, the particle position has been resolved with an accuracy of ±6 nm. For further details regarding the experimental setup, we refer to the supplementary material (SM).

Figure 1(a) shows a schematic of the experimental protocol used in our study. A probe particle is first trapped by an optical tweezers and dragged with constant velocity v through the solution for a time t_{sh}. At time $t = 0$ s, the optical trap is turned off and the particle experiences a recoil opposite to the direction of v along the x-axis. Note that this corresponds to a strong perturbation of the system, which is quite different from previous studies which have been conducted within the linear response regime (e.g. [2, 4, 22]). In figure 1(b) we plotted the results of such an experiment with $v = 3\,\mu\mathrm{m\,s^{-1}}$. The shear time was set to $t_{\mathrm{sh}} = 8$ s which is sufficiently long that the system approaches a non-equilibrium steady state and the recoil amplitude weakly depends on t_{sh}. Note that due to particle sedimentation the particles eventually disappear of the imaging focal plane which limits individual recoil experiments to about ∼10 s. Because of thermal noise, the individual trajectories (colored thin lines) scatter around the corresponding mean value which has been obtained from about 100 repetitions of the protocol (black open symbols). As shown in figure 1(b) and (in) agreement with previous studies, the mean recoil $\langle x(t)\rangle$ is well described by a superposition of two exponential (red plain line) relaxation processes [9]

$$\langle x(t)\rangle = A_{\mathrm{tot}} - A_s \mathrm{e}^{-\frac{t}{\tau_s}} - A_l \mathrm{e}^{-\frac{t}{\tau_l}}, \tag{1}$$

where τ_s and τ_l are two timescales with amplitudes A_s and A_l respectively, and where $A_{\mathrm{tot}} = A_s + A_l$ is the total recoil amplitude. The presence of two timescales is better highlighted in the inset of figure 1(b), where we plotted $\tilde{x}(t) = A_{\mathrm{tot}} - \langle x(t)\rangle$ in a log-normal scale. Before discussing the recoil dynamics in more detail, we note that the appearance of a further (in addition to that of the Maxwell model) relaxation time is not entirely unexpected due to the finite friction of the colloid coupled to the viscoelastic bath.

3. Steady state recoils

To phenomenologically describe the observed recoil behavior we consider a simple model which is shown in figure 1(c). Here, the probe particle with friction coefficient γ is coupled via linear springs with stiffness κ_s and κ_l, respectively, to two bath particles with friction coefficients γ_s and γ_l. Such model corresponds to an extension of the well-known Maxwell model where a single harmonically coupled bath particle is considered, and which is known to provide a good description for the equilibrium properties of viscoelastic fluids [12–14, 23–25].

To rationalize the assumption of a harmonic coupling of the bath particles to the probe, we investigated how A_{tot} varies with v. Within our model, a variation of the shear velocity leads to changes in the elastic forces between the probe and the bath particles, therefore such experiments allow to investigate the properties of the considered springs. From our experiments we observe that all recoil amplitudes A_s, A_l, A_{tot} are proportional to v (figure 2). Notably, the corresponding relaxation times are independent of v (inset of figure 2). As discussed further below, these observations suggest the choice of a linear model, in particular the assumption of linear springs in accordance to figure 1(c).

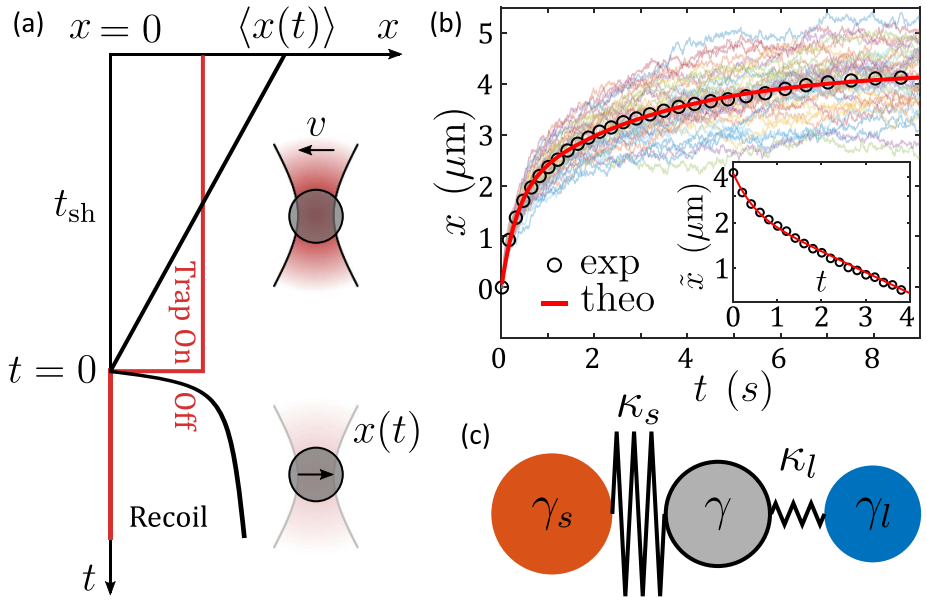

Figure 1. (a) Sketch of a typical recoil protocol. The colloidal probe is first driven by an optical tweezers through the fluid along the x-axis for a time t_{sh} and at a constant velocity v. At $t = 0$ s the optical trap is turned off and the probe is released. Because of accumulated strain in the fluid, the particle performs a recoil opposite to the direction of shear. (b) Typical recoil curves (colored lines) obtained for $t_{sh} = 8$ s and $v = 3\,\mu\text{m s}^{-1}$ and the mean value $\langle x(t) \rangle$ (black circles). The red solid line is a double-exponential according to equation (1) (red line). Inset: $\tilde{x}(t) = A_{tot} - \langle x(t) \rangle$ (A_{tot} corresponds to the total recoil amplitude, see equation (1)) in log-normal scale highlights the two timescales. (c) Sketch of the two-bath particle model where the probe with friction coefficient γ is linearly coupled to two bath particles.

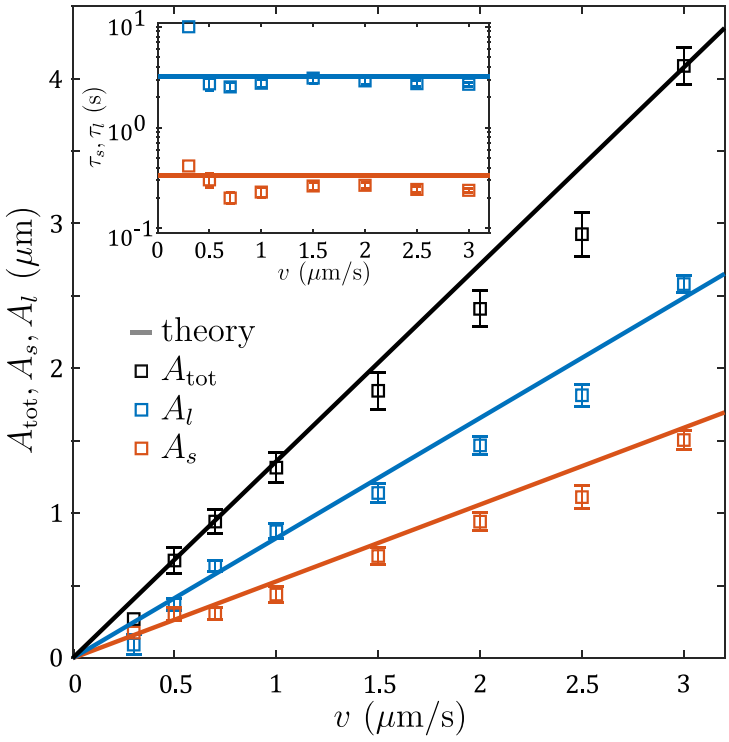

Figure 2. Recoil amplitudes A_{tot} (black), A_s (red), and A_l (blue) as a function of the shear velocity v, for $t_{sh} = 8$ s. The experimental data (squares) are obtained by fitting the individual recoil curves (see figure 1(b)) with equation (1). Theoretical curves (lines) are calculated from equation (9). Inset: relaxation times τ_s (red) and τ_l (blue) extracted from the recoil curves. Square symbols correspond to experiments, and lines to theoretical predictions according to equation (8).

Clearly, the validity of our model is limited to small shear velocities since it does not describe the saturation of A_{tot} at large v, which has been observed in previous studies where shear velocities up to $v = 30\,\mu\text{m s}^{-1}$ were applied [9]. Such saturation results from the finite amount of elastic energy which can be stored in the solvent, an effect which cannot be captured using linear springs. The corresponding linear

Langevin equations describing the dynamics of the probe (at position $x(t)$) and the two bath particles (at positions $x_i(t)$) according to figure 1(c), are given by ($i \in \{s,l\}$)

$$\gamma\dot{x}(t) = -\kappa(t)\left[x(t) - x_0(t)\right] - \sum_i \kappa_i\left[x(t) - x_i(t)\right] + \xi(t) \tag{2}$$

$$\gamma_i\dot{x}_i(t) = -\kappa_i\left[x_i(t) - x(t)\right] + \xi_i(t). \tag{3}$$

The first term on the r.h.s. of equation (2) describes the interaction of the probe with the harmonic optical trap at position

$$x_0(t) = \begin{cases} -vt_{\mathrm{sh}} & , t < -t_{\mathrm{sh}} \\ vt & , -t_{\mathrm{sh}} \leqslant t \leqslant 0 \\ 0 & , t > 0 \end{cases} \tag{4}$$

which is constant for $t < -t_{\mathrm{sh}}$, such that the system is equilibrated at $t = -t_{\mathrm{sh}}$. From $t = -t_{\mathrm{sh}}$ to $t = 0$ the trap is driven with constant velocity v. The time dependent laser trap stiffness $\kappa(t)$ equals κ_{OT} when the trap is on ($t < 0$) and zero when the trap is off. ξ, ξ_s, and ξ_l are independent Gaussian white noises, i.e. for $((\xi_i, \xi_j) \in \{\xi, \xi_s, \xi_l\})$,

$$\langle\xi_i(t)\rangle = 0 \quad , \quad \langle\xi_i(t)\xi_j(t')\rangle = \delta_{ij} 2k_{\mathrm{B}}T\gamma_i\delta(t - t'). \tag{5}$$

We calculate the mean recoil by solving the set of equations (2), (3) and (5) for the mean positions for times $t > 0$ when the probe is released from the optical trap ($\kappa(t) = 0$). The process of shearing the particle through the solvent determines the initial conditions. Due to the large experimental trap stiffness of $\kappa_{\mathrm{OT}} = 32\,\mu\mathrm{N\,m^{-1}}$ we approximate it as fixed-velocity perturbation (hence $x(t) = x_0(t)$). Integrating out equation (3) we obtain for $i \in \{s,l\}$

$$x_i(t) = x(t) - \int_{-\infty}^{t} \mathrm{d}t'\dot{x}(t')\mathrm{e}^{\frac{t'-t}{\tilde{\tau}_i}} + \frac{1}{\gamma_i}\int_{-\infty}^{t} \mathrm{d}t'\xi_i(t')\mathrm{e}^{\frac{t'-t}{\tilde{\tau}_i}}, \tag{6}$$

where $\tilde{\tau}_i = \gamma_i/\kappa_i$ denote the individual relaxation times of the bath particles. After averaging we can insert the protocol of shearing (equation (4)) and find

$$\langle x_i(0)\rangle - \langle x(0)\rangle = v\tilde{\tau}_i\left(1 - \mathrm{e}^{-t_{\mathrm{sh}}/\tilde{\tau}_i}\right). \tag{7}$$

These conditions are inserted into the Mathematica differential equation solver to yield an expression for the mean recoil $\langle x(t)\rangle$.

As a first encouragement, we note that the set of equations (2) and (3) reproduces the experimentally observed dynamics of the probe during the recoil shown in equation (1). The two timescales take the forms

$$\tau_{s,l}^{-1} = \frac{1}{2\gamma}\left[\zeta_s + \zeta_l \pm \sqrt{(\zeta_s + \zeta_l)^2 + 4(\kappa_s\kappa_l - \zeta_s\zeta_l)}\right], \tag{8}$$

where $\zeta_i = (\gamma + \gamma_i)\kappa_i/\gamma_i$. The positive and negative signs correspond to the shorter τ_s and longer τ_l timescales, respectively. Because the two bath particles are mechanically coupled across the probe particle, these timescales depend on the combination of both stiffnesses $\kappa_{s,l}$. The theoretical expressions for the recoil amplitudes are obtained from $\langle x(t)\rangle$ and read

$$\begin{aligned}\frac{A_s}{v} = {} & \frac{\gamma_s\tilde{\tau}_s\left(1 - \mathrm{e}^{-\frac{t_{\mathrm{sh}}}{\tilde{\tau}_s}}\right)}{2\left(\gamma + \gamma_s + \gamma_l\right)}\left[1 + \frac{\tilde{\tau}_l\left[\zeta_l(\tilde{\tau}_l - \tilde{\tau}_s) + \gamma_s + \gamma_l\right]}{(\gamma + \gamma_s + \gamma_l)(\tau_l - \tau_s)}\right] \\ & + \frac{\gamma_l\tilde{\tau}_l\left(1 - \mathrm{e}^{-\frac{t_{\mathrm{sh}}}{\tilde{\tau}_l}}\right)}{2\left(\gamma + \gamma_s + \gamma_l\right)}\left[1 - \frac{\tilde{\tau}_s\left[\zeta_s(\tilde{\tau}_s - \tilde{\tau}_l) + \gamma_s + \gamma_l\right]}{(\gamma + \gamma_s + \gamma_l)(\tau_s - \tau_l)}\right].\end{aligned} \tag{9}$$

A_l follows from A_s by changing indices $s \leftrightarrow l$. Note that equation (9) also holds for finite trap stiffness κ if the shear time t_{sh} is infinitely long.

Fitting the experimental data with equation (1), the extracted experimental recoil timescales $\tau_{s,l}$ and amplitudes $A_{s,l}/v$ are compared to the analytical expressions (8) and (9), which yields the parameters $\gamma_s/\gamma = 1.1$, $\gamma_l/\gamma = 0.88$, $\kappa_s/\gamma = 1.5\,\mathrm{s^{-1}}$, and $\kappa_l/\gamma = 0.2\,\mathrm{s^{-1}}$. In the following, these five parameters are kept constant when we compare theory and experiments, for all the different protocols we applied on the system. Note, that while parameters scale with γ, the absolute parameter values can be obtained through an

independent flow curve experiment (see example in SM) that measures the fluids' viscosity μ, which can then be linked to the total friction in the system: $\gamma + \gamma_s + \gamma_l = 6\pi\mu r$. Lastly, we also compared the mean-square displacement (MSD) of particles passively diffusing in the viscoelastic fluid with the theoretical prediction from our model (obtained from the recoils), and report a very good agreement (see figure 6(a)).

4. Transient regime

To get a deeper understanding on the timescales appearing in transient dynamics of a particle in the viscoelastic fluid, we analyzed the characteristic eigenmodes of the microscopic model (see SM for the full analysis). Interestingly, depending on the presence or absence of the trap, different relaxation modes can arise corresponding to non-reciprocal or reciprocal processes respectively. Indeed, during t_{sh} the probe's position is only determined by the optical tweezers moving at fixed velocity v and not affected by the bath particles. As a result, the interaction between the probe and the bath particles is nonreciprocal: the two bath particles are then fully decoupled leading to their individual relaxation times $\tilde{\tau}_{s,l}$ (upper panel in figure 3). Once the trap is turned off, reciprocity and thus force equilibrium between all three particles must apply, resulting in more complex eigenmodes characterized by the timescales $\tau_{s,l}$ (lower panel in figure 3). These complex timescales are thus the ones we measured in the recoils, which correspond to a reciprocal relaxation of the system.

To confirm the presence of these non-reciprocal relaxation modes experimentally, we have repeated the above experiments for constant $v = 3\,\mu\mathrm{m\,s^{-1}}$, but with t_{sh} being systematically increased. The corresponding recoil amplitudes are shown as a function of t_{sh} in figure 3 (circles). Opposed to the dynamics of the recoil itself which proceeds again via $\tau_s = 0.34$ s and $\tau_l = 3.2$ s, the characteristic timescales of the saturation behavior of the amplitudes vs. t_{sh} are given by the relaxation times of the two uncoupled bath particles, i.e. for a spatially *fixed* probe particle, i.e. $\tilde{\tau}_s = \gamma_s/\kappa_s = 0.7$ s and $\tilde{\tau}_l = \gamma_l/\kappa_l = 4.4$ s, different from $\tau_{s,l}$. Such behavior confirms our eigenmode analysis, and is in perfect agreement with the prediction of our model (solid line). Equation (9) also confirms the experimentally observed t_{sh}-dependence of the amplitudes on $\tilde{\tau}_{s,l}$ (see factors in large round brackets) as shown in figure 3. Notably, A_l is smaller than A_s at small shear time because A_l contains a negative contribution, causing the curve to be rather flat at short time and inflected at later shear times. As a result, in this regime the recoil is largely dominated by just one timescale τ_s.

For an even more direct experimental demonstration of the different relaxation behaviors depending on whether the probe is confined to the trap or not, we have changed our protocol: instead of turning off the optical trap immediately after $t_{\mathrm{sh}} = 8$ s ($v = 3\,\mu\mathrm{m\,s^{-1}}$), it remained on for an additional waiting time t_{w} but with $v = 0$. This allows the bath particles to relax independently towards the fixed probe particle, prior to the recoil where the confined probe provides a coupling between both bath particles (similar to what was done in e.g. [4, 11, 22]). Thus, this process is expected to be fully symmetric to the above loading experiments (figure 3) with the decoupled timescales of the bath particles $\tilde{\tau}_i$ ($i \in \{s, l\}$). Indeed, the measured (triangles) t_{w}-dependent amplitudes of the recoil are in good agreement with the theoretical prediction (solid lines as shown in figure 4). A sketch of the full experimental protocol, with the addition of the waiting time, and the corresponding theoretical derivations and expressions are available in SM.

Because the motion of the bath particles is accessible via equations (2) and (3), for numerical simulations we can also compute the elastic energies stored in the two springs using $E_i = \frac{1}{2}\kappa_i(x_i - x)^2$. The corresponding values are shown in the inset of figure 4 for the above protocol during t_{w} and for the subsequent recoil. As expected, the decay of E_l and E_s is very different during t_{w} compared to the recoil. Opposed to E_l which decreases monotonically, E_s shows a non-monotonic behavior with a minimum around 0.3 s. This is a result of the coupling of the two bath particles (via the probe) during the recoil which leads to a partial exchange of elastic energies between the two relaxation modes.

How can we rationalize the presence of two-time scales in the recoil dynamics? We previously mentioned that the finite coupling between the probe particle and the fluid could be the origin of this additional short timescale. To confirm this hypothesis, we also repeated our experiments for 6 and 7 mM equimolar CPyCl/NaSal concentrations which show a qualitatively identical behavior. As shown in figure 5, when extracting the model parameters, we found that only the properties of one bath particle (κ_l, γ_l) exhibits a strong dependence (more than one order of magnitude) on the micellar concentration while the other model parameters remain rather constant. This observation suggests, that one bath particle describes the coupling of the probe to the network formed by the wormlike micelles, whose mechanical properties strongly depend on the micellar concentration. On the opposite, the other bath particle (κ_s, γ_s) describes the coupling at much smaller displacements of the probe where the network itself is hardly deformed. Under such conditions, only a weak dependence of the parameters on the concentration is expected as confirmed by the weak short-time dependence of the MSD under equilibrium conditions (see figure 6(a)).

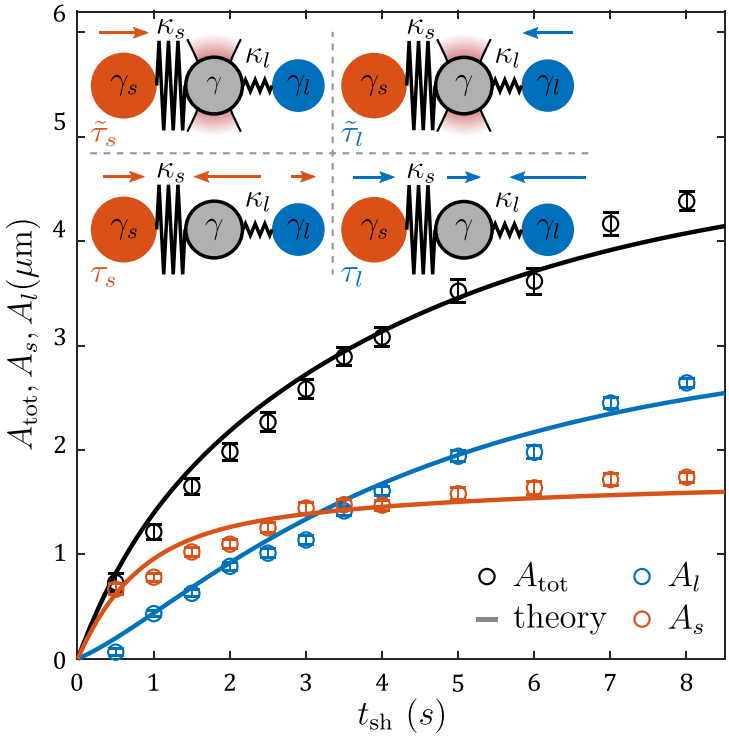

Figure 3. Recoil amplitudes as a function of the shear time $t_{\rm sh}$, for $v = 3\,\mu{\rm m\,s^{-1}}$ for experiments (circles) and theory (lines). For short shearing (small values of $t_{\rm sh}$), the short timescale dominates the recoil dynamics, i.e. $A_s > A_l$. This behavior reverses for long times where $A_s < A_l$, with a cross-over at $t_{\rm sh} \sim 3$ s. Inset: comparison between the eigenmodes associated with $\tilde{\tau}_{s,l}$ (upper panel) when the probe is trapped at a fixed position and with $\tau_{s,l}$ (lower panel), when the probe is free. Since the shearing process is nonreciprocal, there is no coupling between the two bath particles, thus the dynamics for the short and long timescales follow $\tilde{\tau}_{s,l}$.

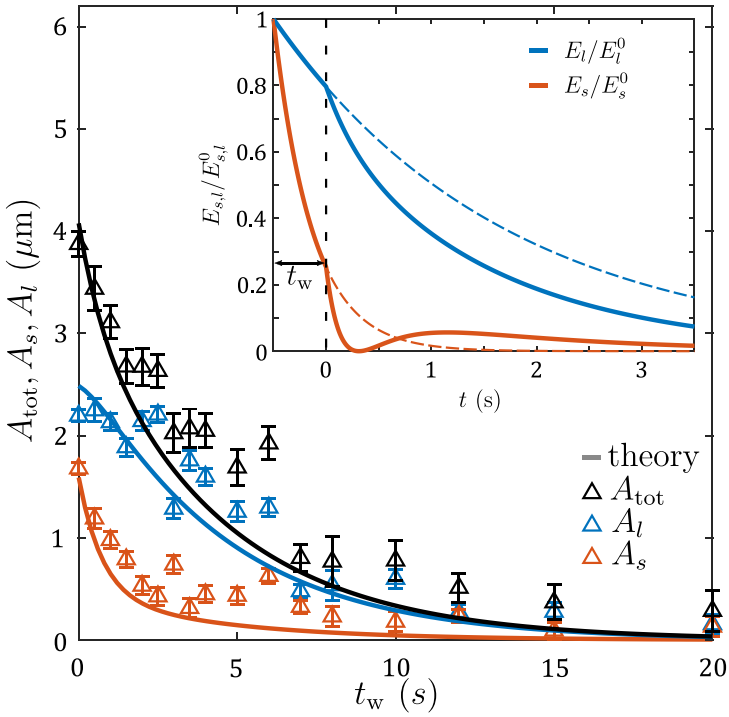

Figure 4. Recoil amplitudes as a function of the waiting time $t_{\rm w}$ and initial conditions $v = 3\,\mu{\rm m\,s^{-1}}$ and $t_{\rm sh} = 8$ s. Experiments and theory are shown as symbols and lines, respectively. A_l always prevails in the recoil behavior, and becomes more dominant when increasing $t_{\rm w}$. Inset: computed (normalized) energy $E_{s,l}/E_{s,l}^0$ values associated with the stiff (κ_s, red lines) and weak (κ_l, blue lines) springs during an experiment with $t_{\rm w} = 0.5$ s. During the time $t_{\rm w}$ the probe is kept at fixed position, and the interactions with the bath particles are nonreciprocal: the relaxation modes thus follow $\tilde{\tau}_{s,l}$. At $t = 0$ s the probe is released in a force-free environment, and the system thus relaxes according to $\tau_{s,l}$. All curves were normalized by $E_{s,l}^0$, the energy associated with each spring prior to the release. Thin dashed lines show a full $\tilde{\tau}_{s,l}$ relaxation process, to better highlight the differences with $\tau_{s,l}$.

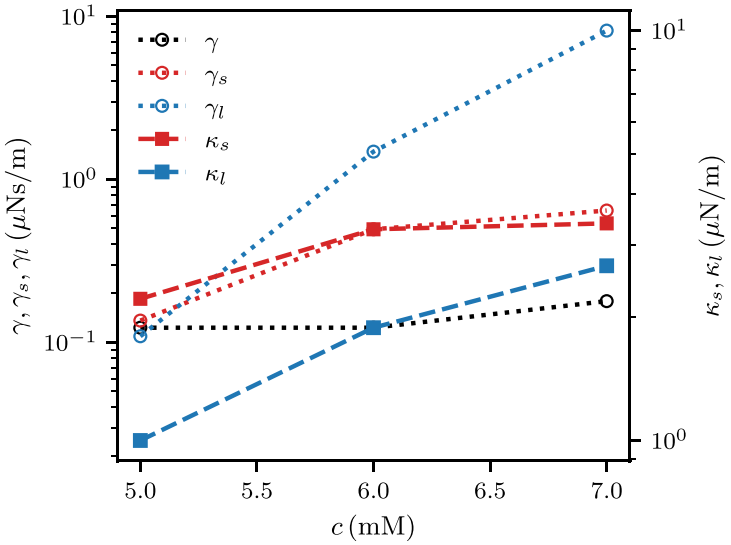

Figure 5. Friction coefficients γ, γ_s, γ_l and coupling strengths κ_s, κ_l in the two-bath particle models fitting experiments at different concentrations c. The parameters associated with the probe and the first bath particle (γ, γ_s, κ_s) stay fairly constant with the fluid concentration. Conversely the parameters associated with the second bath particle (γ_l, κ_l), strongly increase with the fluid concentration.

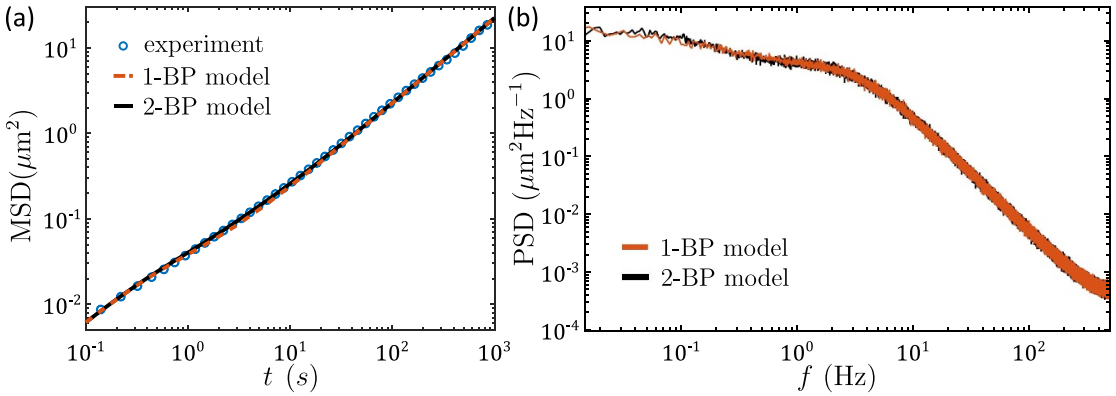

Figure 6. Comparison between one- and two-bath particle models at equilibrium. (a) Mean squared displacement for a freely diffusing particle for experiments (at 5 mM) and theory (see SM for analytical expressions). The experimental data is well described within both models. (b) Power spectral density $\mathrm{PSD}(f) = \langle |x(f)|^2 \rangle_{\mathrm{eq}}$ for simulations (using the parameters obtained from the experiments) of a confined particle. Again the one- and two-bath particle models show nearly identical dynamics at equilibrium.

5. Summary and discussion

As a final remark, we want to mention that recoil experiments provide advantages compared to equilibrium studies when analyzing the properties of viscoelastic materials. Due to the sudden release of accumulated stress acting on the colloidal particle, its motion is less affected by thermal fluctuations which allows to resolve features that could otherwise be easily obscured by (experimental) noise. As an example we have measured the MSD of a passively diffusing probe in our micellar system, and compared it with analytical expressions (see figure 6(a)). While the data is best fitted with our two-bath particle model, a good agreement can also be achieved when only a single-bath particle model is considered (corresponding to a Maxwell model) [17, 26–29]. When looking at the analytical curves, we see that both models exhibit nearly identical MSDs, whereas the additional timescale is clearly observed in the recoil curves. This highlights that such passive measurements are not very sensitive to the system's timescales but are much better resolved (and measured) applying recoil protocols. Similar observations can be made when considering the power spectral density of a trapped particle (see figure 6(b)), where one cannot distinguish between a one- and two-bath particle model.

In summary, we have analyzed the recoil dynamics of a colloidal particle after it was dragged inside an optical trap, through a viscoelastic fluid. For long driving times, when the system has reached its steady state,

we observed the onset of two time scales in the experimental recoil dynamics, which are in excellent agreement with the two eigenmodes of a linearly coupled two-bath particle model. Such linear behavior holds for a remarkably large range of driving velocities, where the measured timescales remain constant. Remarkably, our experiments are also in very good agreement with the model predictions outside of steady state regime, i.e. for partial loading and relaxation. Depending on the specific protocol, either the short or long timescale can be largely suppressed which may explain why single- and double-exponential recoils have been previously observed in different experiments. Additionally, in this study we highlighted the distinction between reciprocal and non-reciprocal protocols, which lead to separate relaxation modes with two sets of timescales. As a result, a particle under free recoil (reciprocal) or trapped inside a strong trap (non-reciprocal) exhibits different relaxation time scales, as was confirmed in our experiments. Yet most experiments using optical tweezers usually lie between these two ideal protocols, in such a situation we thus expect to observe a more complex combination of relaxation modes.

Data availability statement

The data generated and/or analyzed during the current study are not publicly available for legal/ethical reasons but are available from the corresponding author on reasonable request.

Acknowledgment

We thank Matthias Fuchs for fruitful discussions. This project was funded by the Deutsche Forschungsgemeinschaft (DFG), Grant No. SFB 1432—Project ID 425217212. F G acknowledges support by the Alexander von Humboldt foundation.

ORCID iDs

Félix Ginot https://orcid.org/0000-0001-9585-8613
Juliana Caspers https://orcid.org/0000-0001-9495-7118
Karthika Krishna Kumar https://orcid.org/0000-0003-4089-2878
Matthias Krüger https://orcid.org/0000-0001-5015-935X
Clemens Bechinger https://orcid.org/0000-0002-5496-5268

References

[1] Liu J, Gardel M L, Kroy K, Frey E, Hoffman B D, Crocker J, Bausch A R and Weitz D A 2006 *Phys. Rev. Lett.* **96** 118104
[2] Chapman C D, Lee K, Henze D, Smith D E and Robertson-Anderson R M 2014 *Macromolecules* **47** 1181–6
[3] Neckernuss T, Mertens L K, Martin I, Paust T, Beil M and Marti O 2015 *J. Phys.* D **49** 045401
[4] Fitzpatrick R, Michieletto D, Peddireddy K R, Hauer C, Kyrillos C, Gurmessa B J and Robertson-Anderson R M 2018 *Phys. Rev. Lett.* **121** 257801
[5] Ge T, Grest G S and Rubinstein M 2018 *Phys. Rev. Lett.* **120** 057801
[6] Jain R, Ginot F, Berner J, Bechinger C and Krüger M 2021 *J. Chem. Phys.* **154** 184904
[7] Wilking J N and Mason T G 2008 *Phys. Rev.* E **77** 055101
[8] Chapman C D and Robertson-Anderson R M 2014 *Phys. Rev. Lett.* **113** 098303
[9] Gomez-Solano J R and Bechinger C 2015 *New J. Phys.* **17** 103032
[10] Zhou Y and Schroeder C M 2018 *Phys. Rev. Lett.* **120** 267801
[11] Khan M, Regan K and Robertson-Anderson R M 2019 *Phys. Rev. Lett.* **123** 038001
[12] Cates M E and Candau S J 1990 *J. Phys. Condens. Matter* **2** 6869
[13] Spenley N A, Cates M E and McLeish T C B 1993 *Phys. Rev. Lett.* **71** 939–42
[14] Rehage H and Hoffmann H 1988 *J. Phys. Chem.* **92** 4712–9
[15] Jeon J H, Leijnse N, Oddershede L B and Metzler R 2013 *New J. Phys.* **15** 045011
[16] Baiesi M, Iubini S and Orlandini E 2021 *J. Chem. Phys.* **155** 214905
[17] Mason T G and Weitz D A 1995 *Phys. Rev. Lett.* **74** 1250–3
[18] Amblard F, Maggs A C, Yurke B, Pargellis A N and Leibler S 1996 *Phys. Rev. Lett.* **77** 4470–3
[19] Gittes F, Schnurr B, Olmsted P D, MacKintosh F C and Schmidt C F 1997 *Phys. Rev. Lett.* **79** 3286–9
[20] Grebenkov D S, Vahabi M, Bertseva E, Forró L and Jeney S 2013 *Phys. Rev.* E **88** 040701
[21] Crocker J C and Grier D G 1996 *J. Colloid Interface Sci.* **179** 298–310
[22] Robertson-Anderson R M 2018 *ACS Macro Lett.* **7** 968–75
[23] Walker L M 2001 *Curr. Opin. Colloid Interface Sci.* **6** 451–6
[24] Dreiss C A 2007 *Soft Matter* **3** 956
[25] Doerries T J, Loos S A M and Klapp S H L 2021 *J. Stat. Mech. Theor. Exp.* **2021** 033202
[26] Mason T G, Gang H and Weitz D A 1997 *J. Opt. Soc. Am.* A **14** 139–49
[27] van Zanten J H and Rufener K P 2000 *Phys. Rev.* E **62** 5389–96
[28] Lu Q and Solomon M J 2002 *Phys. Rev.* E **66** 061504
[29] van der Gucht J, Besseling N A M, Knoben W, Bouteiller L and Cohen Stuart M A 2003 *Phys. Rev.* E **67** 051106